Trailing Vortex Wind-Tunnel Diagnostics with a Laser Velocimeter

Kenneth L. Orloff*
NASA Ames Research Center, Moffett Field, Calif.

A two-dimensional laser velocimeter whose focal volume can be rapidly traversed through a flowfield has been used to overcome the problem introduced by excursions of the central vortex filament within a wind-tunnel test section. The operation of the instrument is reviewed and data are presented which accurately define the trailing vortex from a square-tipped rectangular wing. Measured axial and tangential velocity distributions are given, both with and without a vortex dissipator panel installed. From the experimental data, circulation and vorticity distributions are obtained and the effect of turbulence injection into the vortex structure is discussed.

Nomenclature

b = wing span
c = wing chord
C_L = lift coefficient
r = radial coordinate from vortex center
u_∞ = wind-tunnel mainstream velocity
v_x = axial velocity component
v_θ = tangential velocity component
$v_{\theta(\max)}$ = maximum tangential velocity
x = streamwise ordinate, aft from trailing edge
z = normal ordinate, above upper wing surface from trailing edge
z_0 = normal location of vortex center
α = angle of attack, deg
Ω = slope of velocity distribution in core region
ζ = vorticity

I. Introduction

WITH an increasing number of large, heavy transport aircraft utilizing the nation's airways and air traffic control system, the probability of hazardous trailing vortex encounters by following aircraft has become alarmingly high. This hazard has been the impetus for both theoretical and experimental research. Experimentally, an accurate quantitative definition of the trailing vortex is important if we are to detail the fluid dynamics of this poorly understood flow. The ultimate goal is to accurately measure the vortex structure and thus be able to theoretically predict the subsequent flow as a function of these measured initial and boundary conditions. Some progress has been made in the measurement of vortex flows by Chigier and Corsiglia[1,2] with hot wire anemometry, and by Mason and Marchman[3] and Logan[4] with pressure probes. Predictions of vortex decay from these initial conditions have been made by Nielsen et al.[5,6] and also by Baldwin et al.[7] and Donaldson and Sullivan.[8]

To alleviate this danger to following aircraft, means have been sought to diffuse the vorticity away from the vortex core so that the rotational velocities will be significantly reduced over the span of the aircraft penetrating the vortex. Such methods as dissipator panels,[9] axial injection,[3,10,11] trailing objects,[12] and various tip modifications[13] have been proposed. Some quantitative velocity measurements are available from which their relative effectiveness as alleviation devices can be assessed, but flow visualization is still heavily relied on. In addition, an evaluation scheme has been applied that employs a trailing model set up in a wind tunnel (downstream of a generating wing) to measure induced rolling moment.[12] While this may be a reasonable means of assessing the hazard of a longitudinal encounter, it is only a static determination and does not define the encounter over a wide range of parameters. In short, to specify the interaction dynamics accurately, one must evaluate dissipation techniques through a precise knowledge of the axial and tangential velocity profiles.

The problem of accurately measuring velocity in trailing vortices must be approached with caution. It is well-known that when objects are inserted into swirling vortex-type flows, upstream influence may alter the flow structure significantly if the flow parameters are in the subcritical regime[14]; the objects may even induce vortex "breakdown" and hence catastrophic decay, which is certainly acceptable as the end, but not the means. However, agreement between recent hot-wire data[15] and laser velocimeter data indicates that the problem of probe interference is not significant for trailing vortices measured to date (see Fig. 2). A more important problem that hinders wind-tunnel vortex measurements has been termed "vortex meander," the lateral (near random) motion of the vortex filament within the wind tunnel itself. This problem of vortex meander has been studied in some detail by Reed.[16] He has determined from photographic data that the scale wavelength of the wind-tunnel turbulence for the NASA-Ames 7- by 10-Foot Wind Tunnel, operating under the conditions reported in the present paper, is between 6 m and 15 m. If one assumes that the turbulence is convected at the mainstream velocity of 25 m/sec, then the characteristic meander period is 0.40 sec for a scale wavelength of 10 m. It is felt that this phenomenon is only physically important insofar as it may simulate the effect of atmospheric turbulence. Nevertheless, this meander requires that the accuracy and reliability of the vortex measurements made with a stationary probe (relative to the wind tunnel) be related to the steadiness and smoothness of the wind-tunnel facility. For a fixed probe, the motion of the vortex requires that time averages be taken, resulting in the loss of detailed structure (particularly near the vortex core). Recent measurements[15] using a high-speed rotating hot wire have demonstrated that this is indeed the case when compared to the earlier time-averaged data of Chigier and Corsiglia.[1,2]

The laser velocimeter (LV) is particularly well suited to making vortex measurements since it does not disturb the flow. Furthermore, the LV processed signal is linearly related to the velocity component sensed and requires no calibration. The importance of these properties of the

Presented as Paper 73-680 at the AIAA 6th Fluid and Plasma Dynamics Conference, Palm Springs, Calif., July 16-18, 1973; submitted October 18, 1973; revision received May 6, 1974.

Index category: Jets, Wakes, and Viscid-Inviscid Flow Interactions.

*Research Scientist. Member AIAA.

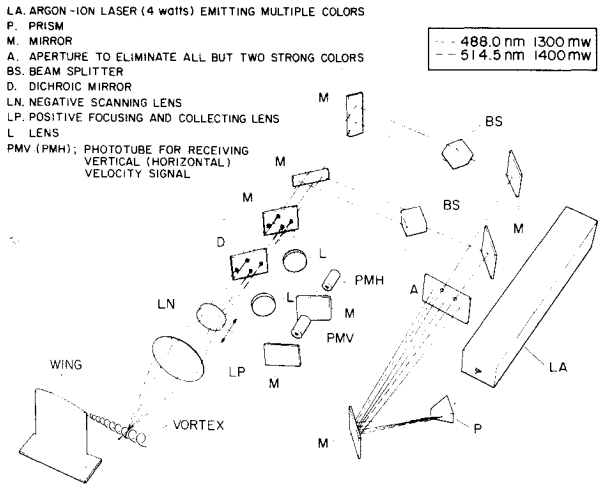

Fig. 1 Schematic diagram of two-color laser velocimeter.

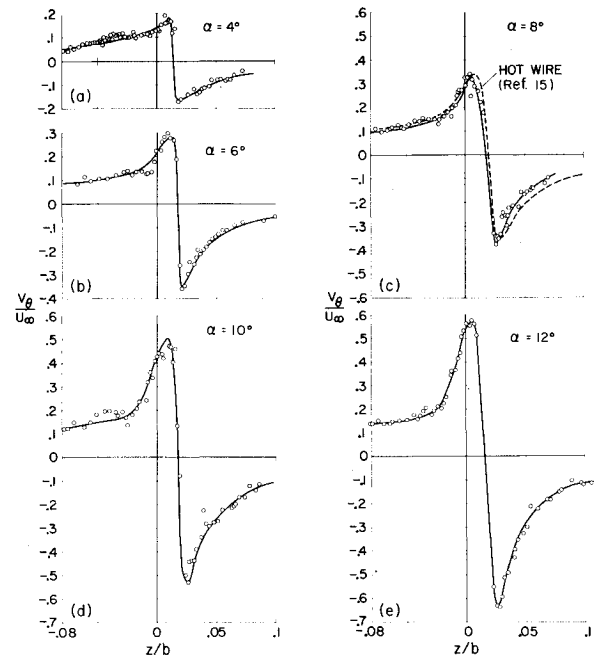

Fig. 2 Tangential velocity profiles for NACA 0015 airfoil at x/c = 2.0, u_∞ = 24 m/sec, for angles of attack of a) 4°, b) 6°, c) 8°, d) 10°, and e) 12°.

laser velocimeter is reflected by simplified testing of different vortex alleviation schemes and the possibility of rapid and complete on-line presentation of the velocity profiles. In addition, such an LV system should be able to measure at least two velocity components simultaneously: a) the axial profile provides information related to the drag increase associated with a particular method of alleviation and b) the tangential velocity profile allows one to evaluate the effectiveness of an alleviation technique. The focal volume of the velocimeter must be able to rapidly traverse the vortex flowfield when acquiring the profile so as to minimize the problem of time averaging due to vortex meander. An LV that meets these criteria has been developed[17] and is briefly described in Sec. II. Its capability of accurately defining the trailing vortex is presented in Sec. III, and its application to the problem of vortex alleviation is reported in Sec. IV.

II. Two-Dimensional Scanning Laser Velocimeter for Vortex Measurements

A two-dimensional laser-velocimeter system has been designed and constructed utilizing the popular dual-scatter, backscatter optical configuration[17] (Fig. 1). Using a two-color technique, simultaneous measurements can be acquired of both the axial and tangential velocities during the time a vortex is being spatially traversed (when an on-diameter penetration is made).

Rapid spatial scanning of the trailing vortex flow is accomplished by the LV system using a simple "zoom-type" lens combination (LN and LP) wherein a small change in the position of the small lens (LN) scans the test point over a much larger distance. The location of this test point within the wind tunnel can be obtained from a voltage representing the linear position of the small lens.

The limits of the spatial scan (for these experiments, between 0.6 and 1.5 m) can be set to encompass the region of interest and it can traverse continuously at speeds up to 1.6 m/sec with automatic reversal at these preset end limits. Since the system operates in a "confocal" mode (same optics used for both transmission and reception), this maximum scan rate is limited only by mechanical constraints and the method of signal processing.

Signal processing was accomplished with two identical HP 8552/8553 spectrum analyzer systems operating at a processing rate of 20 sweeps/sec. For each sweep, the vertical (frequency content display) and horizontal (ramp corresponding to sweep position) outputs of each analyzer were recorded on an oscillograph. The voltage from the linear potentiometer, which is driven by the scanning lens carriage, was also recorded. This voltage (representing the tunnel location of the test point) and the frequency information from the spectrum analyzers are simply reduced to give velocity and location relative to the wing trailing edge (or any other convenient reference). This is the format in which the velocity profiles of the following sections are presented.

Particulate scattering material was introduced into the diffuser section of the wind tunnel by means of a mineral oil smoke generator. Recirculating the air provided a light concentration of the oil vapor throughout the wind tunnel, and LV data could then be gathered throughout the test section except very near the core of the vortex where all but the small, light particles were centrifuged out. However, this centrifugal action distinguishes the core as a much dimmer illumination of the outgoing laser light and allows one to specify when an "on-diameter" traversal has been accomplished. Such a traversal is only considered valid if, during the traversal, the vertical location of the vortex core remains aligned with the two outgoing laser beams which define the horizontal plane. A small amount of core motion is acceptable when the probe volume of the velocimeter is well outside the central region where the tangential velocity gradient is low. The vortex must, however, remain nearly stationary as the probe volume traverses the core region for the traversal to be considered acceptable.

III. Vortex Definition

To demonstrate the utility of the laser velocimeter in precisely defining the axial and tangential velocity profiles, detailed measurements of velocity distributions have been made in the vortices generated by a square-tipped, 0.457-m chord (c), 1.218-m semispan ($b/2$) wing mounted in the NASA Ames 7- by 10-Foot Wind Tunnel. The airfoil section is NACA 0015 and the planform is rectangular with no twist. The vortex generated by this wing at 12° angle of attack has previously been studied by Chigier and Corsiglia[1,2] and a comparison with LV results is given in Ref. 18.

For definition purposes, a detailed survey was made of this vortex two chord lengths behind the wing (x/c = 2.0). The capability of the LV system to accurately measure

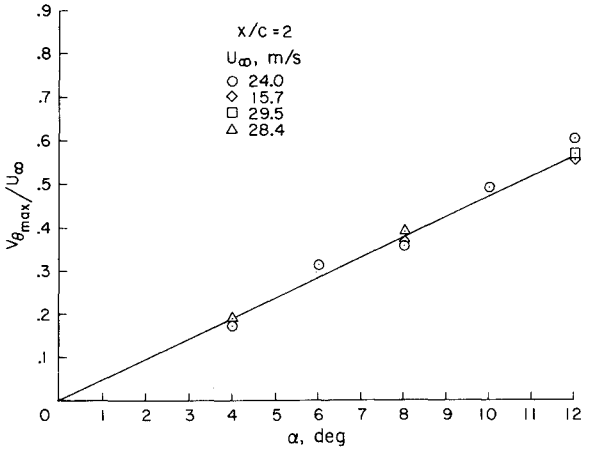

Fig. 3 Dimensionless maximum tangential velocity, $v_{\theta(max)}/u_\infty$ vs angle of attack, α, for NACA 0015 airfoil.

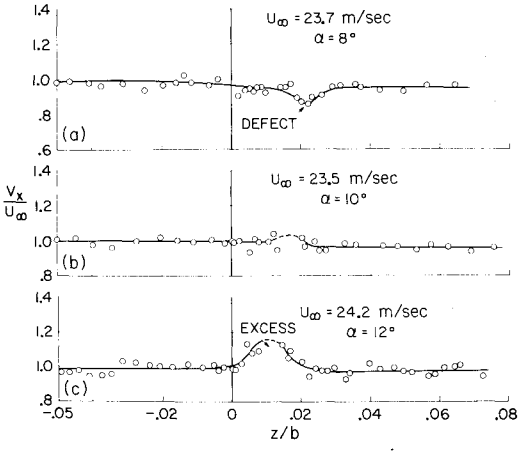

Fig. 4 Axial velocity profiles for NACA 0015 airfoil at x/c= 2.0. a) α = 8° taken simultaneously with Fig. 2 c; b) α = 10° taken with Fig. 2 d; and c) α = 12° taken with Fig. 2 e.

these profiles is demonstrated in Fig. 2. These data represent "slow" scanning of the vortex at an average spatial speed of about 15 cm/sec which was necessary in order to obtain sufficient detail within the core region for the fixed processing rate (20/sec) of the spectrum analyzer. There is obvious scatter in the data due to the movement of the vortex during a traversal. Core detail is obtained, however, since the traversal time across the core (approximately 0.3 sec) is less than the characteristic meander period of 0.4 seconds. The profile measured for an angle of attack of 8° is seen to be in agreement with that reported by Consiglia et al.[15] for a full span model which is geometrically identical.

This model generated a vortex whose core diameter is observed (Fig. 2) to be about 3% of the span, or about 7.3 cm. Since the length of the LV probe volume is approximately 0.2 cm, it is clear that spatial resolution of the velocity distribution is satisfactory. It is only in the very center of the vortex (region of rigid rotation) that some question may exist as to the effect of a velocity gradient across the probe volume. This question is difficult to resolve since too few scattering particles were present in the vortex core to produce an adequate signal.

The maximum tangential velocity for a given angle of attack is said to be the average maximum of the two peaks of Fig. 2. If this maximum, $v_{\theta(max)}/u_\infty$, is plotted against the angle of attack, then, for this simple wing, one might expect such a graph to be linear. This is indeed the case, as shown in Fig. 3. Note that the data extrapolate well to the origin, as they should. Moreover, it is significant that the additional points plotted for various fretream velocities also fall on this line, for it implies that over the range of tunnel speed indicated in Fig. 3, there appears to be no dependence on Reynolds number. This greatly simplifies the task of data acquisition, as one need not be concerned with the *exact* tunnel speed at which a traversal is made. The most significant parameters are configuration and angle of attack.

Axial velocity profiles measured simultaneously are given in Fig. 4 for angles of attack of 8°, 10°, and 12°. At 8°, there is a very small axial velocity defect in the core region. At 10°, the defect has disappeared or has, at best, become only a small excess. At 12°, the axial velocity excess is pronounced. This phenomenon has also been observed by Chigier and Corsiglia,[1,2] and a reasonable explanation concerning the relationships between total head loss, induced drag, parasite drag, etc., has been given by Batchelor.[19]

This type of velocity definition is meaningful in that the tangential profile can now be used to calculate rolling moments and other dynamic interactions; the axial profile is related to the model drag and total head loss. Using both profiles for initial conditions, it should also be possible to make some assertions as to the subsequent development of the vortex.[5,6] Equally important, this kind of accurate velocity definition now provides for a comparative evaluation of suggested vortex alleviation schemes.

IV. Vortex Alleviation

The use of vortex dissipator panels was investigated by Corsiglia, Jacobsen, and Chigier[9] as a possible means of vortex alleviation. With the laser velocimeter, a number of these panels has been tested on the wing described in Sec. III. Studies have been made for angles of attack of 8°, 10°, and 12° for each panel, but only the results for a single panel at 12° are presented here to shorten the discussion.

A square panel that is 4% of the semispan (11% of the wing chord) was installed at the wing tip at the 1/4-chord position (Fig. 5). The resulting axial and tangential velocity distributions are presented in Fig. 6. The axial velocity excess (Fig. 4) has been removed and a large defect is present. This defect is intimately related to the added drag on the wing (as discussed by Batchelor[19]). Examination of the tangential profile reveals a decrease in $v_{\theta(max)}/u_\infty$ of about 20% from that of the clean configuration (Fig. 2e). However, from the data of Corsiglia et al.,[9] a reduction of about 4% is expected in C_L merely because of the decrease in lift with the panel attached. Hence,

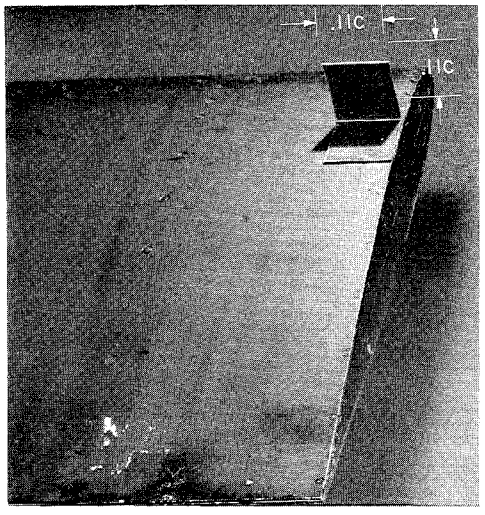

Fig. 5 Dissipator panel mounted at tip of airfoil at 1/4 chord position.

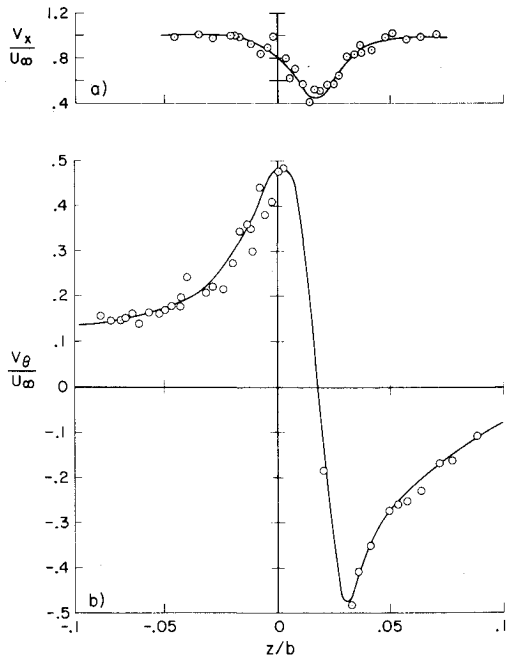

Fig. 6 Velocity distributions with dissipator panel at wing tip. $x/c = 2.0$, $\alpha = 12°$, $u_\infty = 22.4$ m/sec; a) axial and b) tangential.

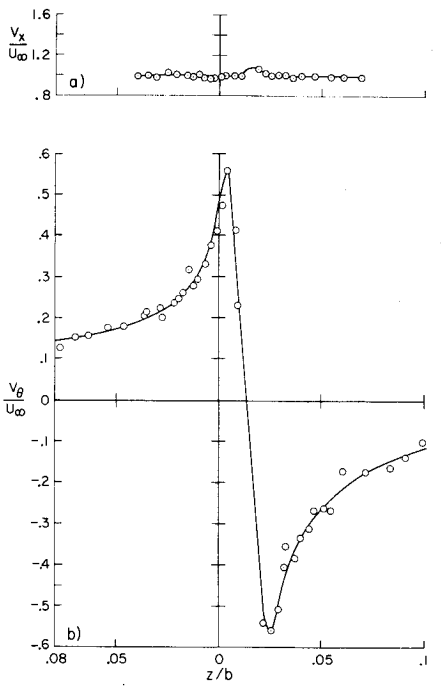

Fig. 8 Velocity distributions with dissipator installed at wing tip. $x/c = 7.0$, $\alpha = 11.1°$, $u_\infty = 24.3$ m/sec; a) axial and b) tangential.

there should be a similar 4% decrease in $v_{\theta(\max)}/u_\infty$ from this effect alone. Therefore, it can be concluded that there is only about a 16% reduction in $v_{\theta(\max)}/u_\infty$ which is not associated with a loss of lift.

These results do not agree with the 50% reductions reported by Corsiglia et al.[9] at a downstream distance of $x/c = 10$. It was therefore necessary to obtain LV data at a station further downstream. Unfortunately, at $x/c = 7.0$, data were obtained for an angle of attack of 11.1° rather than 12°, but many conclusions can still be made regarding vortex development from $x/c = 2.0$ to $x/c = 7.0$.

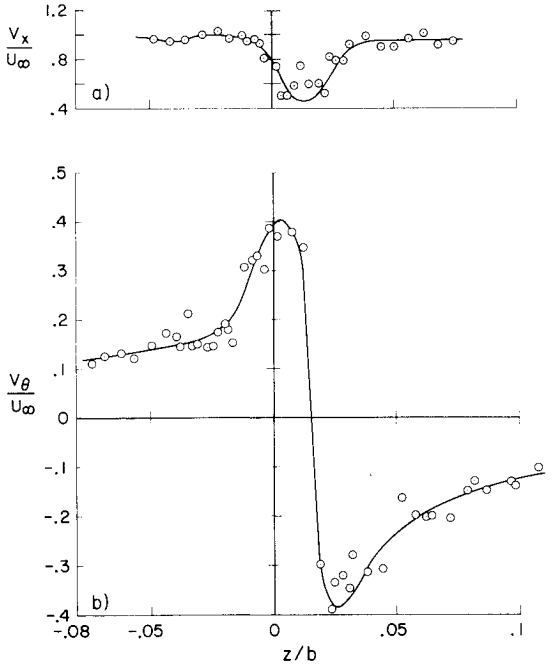

Fig. 7 Velocity distributions for clean configuration (no dissipator). $x/c = 7.0$, $\alpha = 11.1°$, $u_\infty = 24.6$ m/sec; a) axial and b) tangential.

Figure 7 shows the resulting profiles for the clean configuration (no dissipator) at $x/c = 7.0$ and $\alpha = 11.1°$; $v_{\theta(\max)}/u_\infty$, observed to be about 0.56, compares favorably with a value of 0.53 (at $\alpha = 11.1°$) taken from Fig. 3 at $x/c = 2.0$. Therefore, it appears that within five chord lengths no dissipation has occurred. In addition, the axial excess is in agreement with the trend established in Fig. 4.

The distributions at $x/c = 7.0$ with the dissipator panel installed are shown in Fig. 8. The axial defect profile is nearly identical to that at $x/c = 2.0$. Now, however, the tangential profile shows a pronounced reduction in $v_{\theta(\max)}/u_\infty$ by about 26% (after a 4% correction for C_L).

Figure 9 is a summary of these results, which are compared with results obtained from tests of a geometrically similar configuration in the Ames 40 × 80-Foot Wind Tunnel where values of $x/c = 55$ were obtained.[15] From these results, the mechanism that alleviates the vortex appears to develop with increasing downstream distance, with very little effect (except drag in the axial profile) near the wing. It is hypothesized that the presence of these panels introduces, as the vortex forms, large amounts of turbulence into the core area in the form of

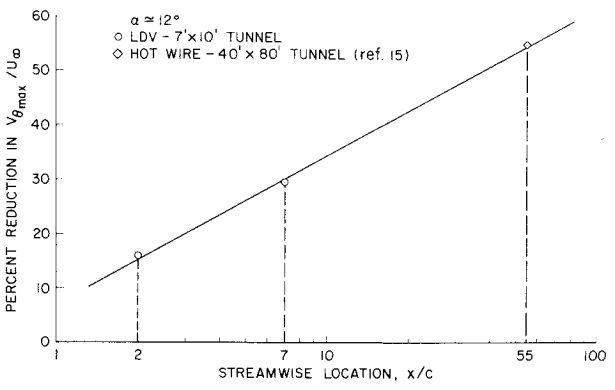

Fig. 9 Streamwise development of dissipator alleviation technique.

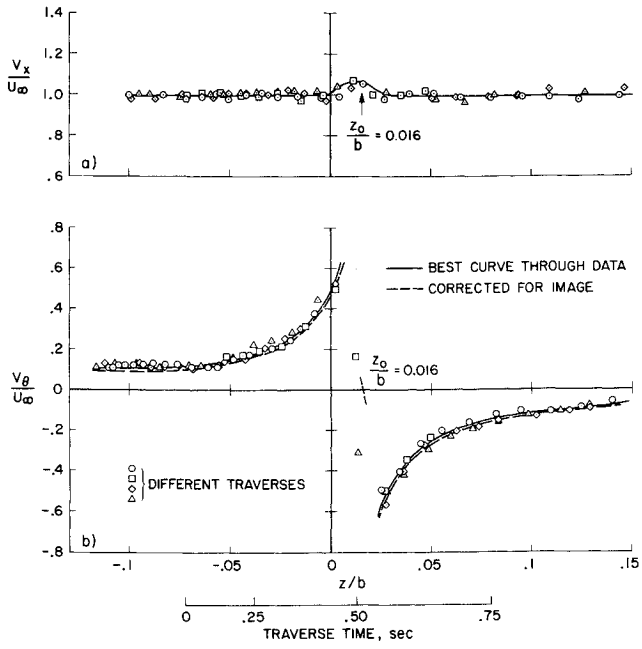

Fig. 10 Velocity distributions from high-speed traverses—clean configuration. $x/c = 7.0$, $\alpha = 11.1°$, $u_\infty = 22.8$ m/sec; a) axial and b) tangential.

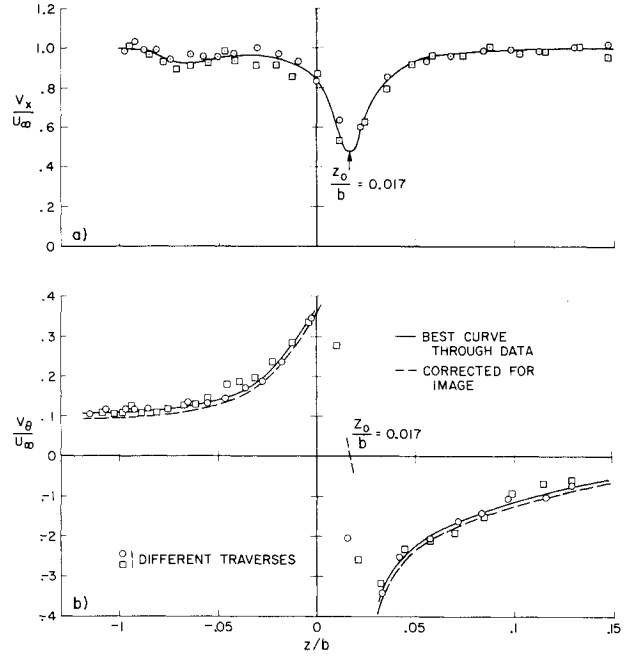

Fig. 11 Velocity distributions from high-speed traverses—dissipator installed. $x/c = 7.0$, $\alpha = 11.1°$, $u_\infty = 22.2$ m/sec; a) axial and b) tangential.

large eddies (on the order of the size of the panel). The cascading of these eddies to the microscale transfers momentum, resulting in dissipation. These ideas are not new and other investigators[10,11,13,20] have suggested that introducing turbulence into the vortex by virtually any means is a dominant factor in reducing the tangential velocity.

For a more meaningful discussion of this turbulence injection technique, one must know how the vorticity is distributed throughout the vortex (i.e., circulation as a function of radius). To obtain data for use in determining the circulation curve, a high spatial scan rate is necessary to traverse the vortex core in a time short compared to the characteristic meander time, to insure that the region of high velocity gradient near the center of the vortex remains stationary during a traversal. With a spectrum analyzer processing rate of 20 sweeps/sec, detail over short distances (through the core area) is lost. However, if several high-speed traversals are made, then a good mean curve may be drawn which is *not* a spatial average.

The velocity distributions obtained from the clean configuration are shown in Fig. 10. Mean curves are drawn as the average of the four traverses. Nearly the entire vortex is traversed in less than 1.0 sec. The central region of high velocity gradient is crossed in a time less than the characteristic meander time of 0.40 sec. The curve in Fig. 10b, includes a correction for the influence† of an image vortex that results from the proximity of the wall through which the laser measurements are taken. The errors introduced into the circulation distribution by neglecting this correction can become pronounced at large radii due to an increasing contribution of the image below the wing (which is nearest the wall). For example, from Fig. 10, the image correction is nearly 20% of the measured velocity at $z/b = -0.1$, which would, in turn, affect the circulation by 20%. Similarly, the velocity profiles with the dissipator installed are shown in Fig. 11. Note that the axial profiles of Figs. 10a and 11a are identical to those of Figs. 7a and 8a, respectively. There also appears to be a slight velocity defect in Figs. 8a and 11a below the wing which is not understood.

Figures 10b and 11b both suggest an asymmetry of the profile for distances, r/b, greater than 0.05. This same phenomenon has been observed by Chigier[21] and Lezius,[22] with a consistent pattern of higher circumferential velocities (for a given r/b) below the wing than are encountered above the wing (even after the image correction has been made). It is assumed that, to a first approximation, the circulation is the average value of the two sides. The vortex center is determined from the data nearest the core by requiring that $r_+v_+ = r_-v_-$, so that for a given v, say $v_+ = v_- = 0.40$, the center is at $z_0/b = 1/2[(z_+ + z_-)/b] = 1/2\,(0.036 - 0.004) = 0.016$ (for a clean configuration).

The resulting circulation distribution is presented in Fig. 12. The theoretical value of the circulation is deter-

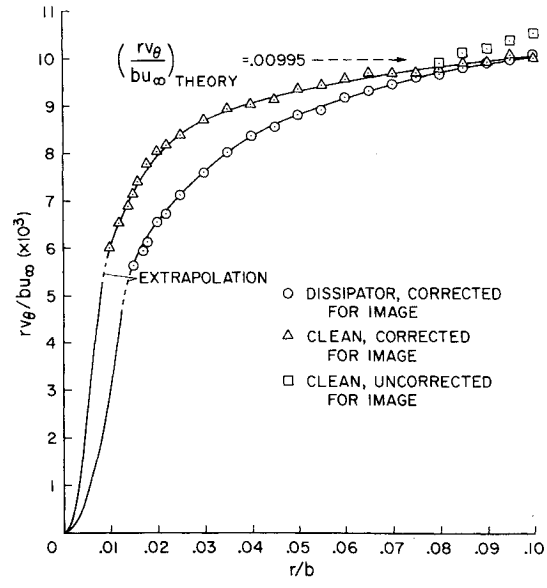

Fig. 12 Radial distribution of circulation showing effect of dissipator.

†This influence is not a "real" effect, as opposed to the image vortex which represents the opposite wing tip.

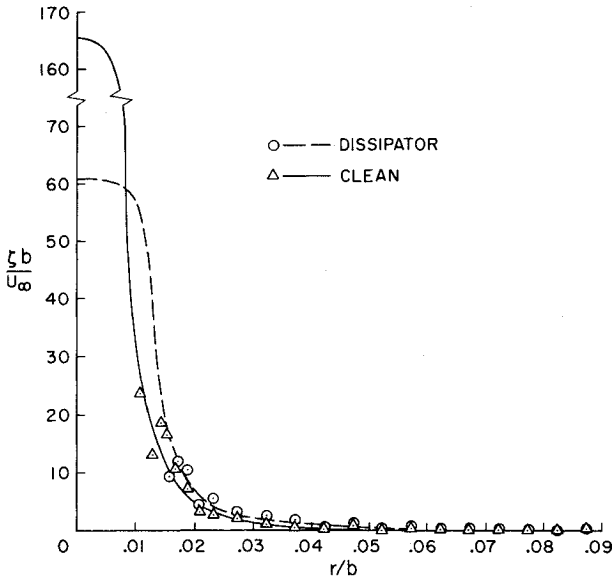

Fig. 13 Radial distribution of vorticity.

mined using the known lift coefficient, $C_L = 0.666$ for $\alpha = 11.1°$. Some data points have also been included for the uncorrected (for the image) vortex at large radii from Fig. 10b. Clearly, one must correct for this image if convergence to the theoretical value is to be obtained. Furthermore, the data can be extrapolated a short distance at lower radii into the core region. For the rigid core, the circulation is given by $K = rv_\theta = \Omega r^2$, where Ω is the slope of the velocity distribution in this region. Hence, since the parabolic curve that contains the end point of the extrapolation is unique (Fig. 12), Ω is determined. The vorticity can be computed from $\zeta = (1/r)(\partial rv_\theta/\partial r)$ and is given in Fig. 13. In the core region, it is merely equal to 2Ω. It appears that the dissipator panel has moved some vorticity radially outward so as to conserve angular momentum, and the regions affected by this redistribution due to the effects of turbulence injection can be accurately specified.

V. Conclusion

The use of a unique laser velocimeter with high-speed spatial scanning capability has been described and its direct application to trailing vortex wake turbulence research has been presented. The scanning feature of this instrument minimizes the difficulties in velocity measurement due to what has been termed "vortex meander." Accurate vortex definition is achieved and the data are repeatable and consistent with other experimental results.[15]

The results presented are not intended necessarily to advocate the use of dissipator panels for vortex alleviation, but only to demonstrate the utility of the laser velocimeter in quantitatively assessing the relative effectiveness of any particular alleviation device. Furthermore, the LV system has been used to suggest the manner in which turbulence generated by the dissipator is incorporated into the vortex structure.

References

[1]Chigier, N. A. and Corsiglia, V. R., "Tip Vortices—Velocity Distributions," TM X-62,087, 1971, NASA.

[2]Chigier, N. A. and Corsiglia, V. R., "Wind-Tunnel Studies of Wing Wake Turbulence," *Journal of Aircraft*, Vol. 9, No. 12, Dec. 1972, pp. 820–825.

[3]Mason, W. H. and Marchman, J. F., III, "Farfield Structure of an Aircraft Trailing Vortex, Including Effects of Mass Injection," CR-62078, 1972, NASA.

[4]Logan, A. H., "Vortex Velocity Distributions at Large Downstream Distances," *Journal of Aircraft*, Vol. 8, No. 11, Nov. 1971, p. 930.

[5]Nielsen, J. N. and Kuhn, G. D., "Analytical Studies of Aircraft Trailing Vortices," AIAA Paper 72-42, San Diego, Calif., 1972.

[6]Nielsen, J. N. and Schwind, R. G., "Decay of a Vortex Pair Behind an Aircraft," in *Aircraft Wake Turbulence and Its Detection*, 1st ed., Plenum Press, New York, 1971, pp. 413–454.

[7]Baldwin, B. S., Chigier, N. A., and Sheaffer, Y. S., "Prediction of the Far Flowfield in Trailing Vortices," *AIAA Journal*, Vol. 11, No. 12, Dec. 1973, pp. 1601–1602.

[8]Donaldson, C. DuP. and Sullivan, R. D., "Decay of an Isolated Vortex," *Aircraft Wake Turbulence and Its Detection*, 1st ed., Plenum Press, New York, 1971, pp. 389–411.

[9]Corsiglia, V. R., Jacobsen, R. A., and Chigier, N. A., "An Experimental Investigation of Trailing Vortices Behind a Wing with a Vortex Dissipator," *Aircraft Wake Turbulence and Its Detection*, 1st ed., Plenum Press, New York, 1971, pp. 229–242.

[10]Mason, H. W. and Marchman, J. F., III, "The Farfield Structure of Aircraft Wake Turbulence," AIAA Paper 72-40, San Diego, Calif., 1972.

[11]Poppleton, E. D., "Effect of Air Injection into the Core of a Trailing Vortex," *Journal of Aircraft*, Vol. 8, No. 8, Aug. 1971, p. 672.

[12]Patterson, J. C., Lift Induced Wing-Tip Vortex Attenuation," *Journal of Aircraft*, to be published.

[13]Marchman, J. F., III and Uzel, J. N., "Effect of Several Wing Tip Modifications on a Trailing Vortex," *Journal of Aircraft*, Vol. 9, No. 9, Sept. 1972, p. 682.

[14]Orloff, K. L., "Experimental Investigation of Upstream Influence in a Rotating Flowfield," Ph.D. thesis, June 1971, Dept. of Mechanical Engineering. University of California at Santa Barbara.

[15]Corsiglia, V. R., Schwind, R. G., and Chigier, N. A., "Rapid Scanning, Three-dimensional Hot Wire Anemometer Surveys of Wing Tip Vortices," *Journal of Aircraft*, Vol. 10, No. 12, Dec. 1973, p. 752.

[16]Reed, R. E., "Properties of the Lateral Random Oscillations of Trailing Vortices Observed in Wind-Tunnel Tests," TR 47, 1973, Nielsen Engineering and Research, Inc., Mountain View, Calif.

[17]Grant, G. R. and Orloff, K. L., "A Two-Color Dual-Beam Backscatter Laser Doppler Velocimeter," *Applied Optics*, Vol. 12, Dec. 1973, p. 2913.

[18]Orloff, K. L. and Grant, G. R., "The Application of Laser Doppler Velocimetry to Trailing Vortex Definition and Alleviation," TM X-62,243, 1973, NASA.

[19]Batchelor, G. K., "Axial Flow in Trailing Line Vortices," *Journal of Fluid Mechanics*, Vol. 20, 1964, pp. 645–658.

[20]Kantha, H. L., Lewellen, W. S., and Durgin, F. H., "Response of a Trailing Vortex to Axial Injection into the Core," *Journal of Aircraft*, Vol. 9, No. 3, March 1972, p. 254.

[21]Chigier, N. A., "Experimental Studies of Aircraft Wake Turbulence," 14th Israel Annual Conference on Aviation and Astronautics, 1972.

[22]Lezius, D. K., "Water Tank Study of the Decay of Trailing Vortices," *AIAA Journal*, Vol. 12, No. 8, Aug. 1974, pp. 1065–1071.